SIMULATION OF TRANSPORT PHENOMENA IN InP

Received 11/06/2003 – Accepted 31/12/2004

Abstract

In the present work we report results of the simulation of transport phenomena in InP under uniform electric fields in both transient and steady state regimes using semi-classical Ensemble Monte Carlo method (EMC). The EMC algorithm used consists mainly of the simulation of an ensemble of carriers and follows their history in parallel for a sequences of very short time intervals in three dimensional momentum and real spaces. After each sampling interval, data (drift velocity, energy…) is collected for each particle and the values are averaged. In our simulation an ensemble of 10^5 electrons are used. The program was written with Fortran 90 language and run on IBM PC(PIII, 800GHz). The obtained results are in good agreement with reported experimental data.

***Key words**: Transport phenomena, Monte Carlo, semiconductor, scattering.*

Résumé

Dans ce travail, on présente les résultats de la simulation du phénomène de transport dans l'InP, avec la méthode semi-classique de l'Ensemble Monte Carlo (EMC). L'étude de l'influence d'un champ électrique uniforme en régimes transitoire et stationnaire a été effectuée. L'algorithme EMC utilisé repose essentiellement sur la simulation du mouvement des porteurs de charge en parallèle pour des intervalles de temps réguliers très court dans l'espace des vecteurs d'onde et l'espace réel. A la fin de chaque intervalle l'historique des particules (énergie, vitesse de dérive..) est enregistré, ainsi les valeurs moyennes sont calculées. On a considéré un échantillon d'InP non-dopé composé de10^5 électrons. Les calculs on été fait sur IBM PC(PIII, 800GHz à l'aide d'un code Fortran 90. Les résultats obtenues sont en bon accord avec les données expérimentales.

***Mots clés**: phénomène de transport, Monte Carlo, semi-conducteur, collision.*

A. BELGHACHI
Laboratory of Semiconductor Devices Physics
Physics Department
University of Béchar (Algeria)

ملخص

أجرينا في هذا البحث محاكاة لظاهرة التنقل في **InP** تحت تأثير حقل كهربائي متجانس وذلك خلال المرحلتين الانتقالية والمستقرة باستعمال طريقة مونتي كارلو (EMC). يعتمد الخوارزمي المستعمل أساسا على محاكاة حركة متوازية لحوامل الشحنة خلال مجالات زمنية منتظمة وقصيرة جدا في الفضاءين الشعاعي الموجي والحقيقي، في نهاية كل مجال يسجل تاريخ كل جزيئة (سرعة الانسياق، الطاقة...) ثم تحصيل المعدلات. تتكون العينة المستعملة من 10^5 إلكترون. كتب البرنامج المستعمل بلغة الفورتران (Fortran 90) وأنجز من خلال جهاز IBM PC(PIII, 800GHz). إن النتائج المتحصل عليها في انسجام جيد مع المعطيات التجريبية الواردة.

***الكلمات المفتاحية**: ظاهرة التنقل، مونتي كارلو، شبه ناقل، الإنتشار .*

The advance of epitaxial technologies such as molecular beam epitaxy (MBE) and metal-organic chemical vapour deposition (MOCVD), has lead to an extraordinary dimensional control of semiconductor layers. It has enabled the fabrication of unconventional device structures such as modulation-doped layers, superlattices, quantum wells...etc with new properties resulting from the controllability of band discontinuities and the confinement of electronic states to narrow layers. At the same time advent of modern time resolved measurement techniques, such as the electo-optic sampling (EOS) technique, allows transport processes to be determined with sub-picosecond temporal resolution. In modelling such device structures and their transport processes, hot electrons as well as time and space dependent phenomena are important. It is invalid to assume a priori the carrier distribution functions, as used in common numerical models such as drift-diffusion equations, relaxation time approximations, displaced Maxwellian approaches, etc. The Monte Carlo (MC) technique, besides its greater ability to deal with band and scattering details, has the advantage of solving the Boltzmann transport equation (BTE) without assuming a priori distribution functions [1,2].

I- MONTE CARLO SIMULATION

The MC technique involves basically simulating the free particle motion terminated by instantaneous random scattering events. The MC algorithm consists of generating random free flight times for each particle, choosing the type of scattering occurring at the end of the free flight, changing the final energy and momentum of the particle after scattering and then repeating the procedure for the next free flight [3,4]. Sampling the particle motion at various times throughout the simulation allows for the statistical estimation of physical quantities such as the

distribution function, the average drift velocity, the average energy, the valley occupancy, etc.

The simulation starts with one electron in given initial conditions with wave vector k_0. Then the duration of the first free flight is chosen with a probability distribution determined by the scattering probabilities. During the free flight the applied force changes the momentum of the electron according to the relation:

$$k(t) = k(0) - \frac{eEt}{\hbar} \tag{1}$$

where E is the electric field vector component directed in x, y or the z direction.

If $\Gamma[\boldsymbol{k}(t)]$ is the total scattering rate given by the sum of all individual scattering rates:

$$\Gamma(k) = \sum_{i=1}^{m} \lambda_i(k) \tag{2}$$

where m is the total number of scattering mechanism and $\lambda_i(k)$ is the individual scattering rate.

Then the probability per unit time that the electron will drift before a scattering event is given by:

$$P(t) = \Gamma\left[k(t)\right] \exp\left\{ -\int_0^{tf} \Gamma\left[k(t)\right] dt \right\} \tag{3}$$

The time of free flight t_f can be obtained by integrating equation (3):

$$r = 1 - \exp\left[-\int_0^{tf} \Gamma\left[k(t)\right] dt \right] \tag{4}$$

where r is a random number uniformly distributed between 0 and 1. Equation (4) is the fundamental expression used to generate the random free flight time after each scattering event. This equation is complicated and would require extensive computer resources to solve, as flight times are generated millions of times in a standard MC simulation. However, the so-called self-scattering method devised by Rees [5] can be used. In Rees' method we introduce a fictitious scattering mechanism whose scattering rate always adjusts itself in such a way that the total rate (self-scattering plus real scattering) is a constant in time:

$$\Gamma_0 = \lambda_0(k) + \Gamma(k) \tag{5}$$

where $\lambda_0(k)$ is the self scattering rate and Γ_0 is constant. The integration of equation (3) gives then:

$$t_f = -\frac{1}{\Gamma_0} \ln(1 - r) \tag{6}$$

since $r \in (0,1)$ we can also write:

$$t_f = -\frac{1}{\Gamma_0} \ln(r) \tag{7}$$

It is necessary, however, to take the constant Γ_0 to be at least as large as the largest value of $\Gamma[k(t)]$ in order to avoid negative values of $\lambda_0(k)$. When $\Gamma(\varepsilon)$ is an increasing function of ε, as is often the case, Γ_0 can be taken equal to $\Gamma(\varepsilon_M)$, where ε_M is a maximum electron energy with negligible probability of being achieved by the electron during the simulation. The value of ε_M cannot be taken too large in order to avoid unnecessarily large value of Γ that would result in a waste of computer time for self-scattering events.

To reduce the probability of self-scattering events we adopted a so called iterative Gamma [6]. In this technique the first estimated Γ_0 is Γ_{01} that should be greater than $\Gamma(\varepsilon_1)$, ε_1 is the electron energy at the start of the flight. At the end of the flight the electron has a new energy ε_2 . If $\Gamma(\varepsilon_2)$ is greater than Γ_{01}, scattering mechanisms are excluded from the choice yielding a negative scattering rate which we have to avoid. A new selection has therefore to be made with:

$$\Gamma_{02} = \Gamma_{01} + \Delta\Gamma_0 \tag{8}$$

If $\Gamma_{02} < \Gamma(\varepsilon_2)$ the process has to be repeated by adding an other increment $\Delta\Gamma_0$ to Γ_{02} . This process usually converges after a few steps. The selection of $\Delta\Gamma_0$ is a matter of experienced in our case $\Delta\Gamma_0 = 0.1\ \Gamma_0$ was a reasonable choice.

The effectiveness of the procedure depends critically on the additional computation time required by the calculation of the free flight compared to the time saved through the reduction of self-scattering events.

To determine the scattering process, the product of a random number $r \in (0,1)$ with Γ_0 is compared with the successive sums of the individual scattering rates $\sum_{i=1}^{m} \lambda_i(k)$, where m is the total number of real scattering mechanisms. If $\sum_{i=1}^{j-1} \lambda_i(k) \le r\Gamma_0 < \sum_{i=1}^{j} \lambda_i(k)$ the j^{th} scattering is selected while for $r\Gamma_0 > \Gamma(\varepsilon)$ this corresponds to self-scattering.

In MC simulation, a quantity A is in general a function of free flight duration, ensemble size, valley, position, and time. The average value (e.g., the drift velocity, the mean energy, etc.) is given by:

$$< A >= \frac{1}{N} \sum_{i=1}^{N} A_i\left[k(t)\right] \tag{9}$$

where N is the number of particles in the ensemble.

We may also obtain the electron distribution function for a homogeneous system in steady-state. To do so a mesh in k space (or energy) is set up at the beginning of the computer run. The steady-state distribution function is proportional to the number of electrons that at time t are found to be in a cell of fixed volume Δk around k (or $\Delta\varepsilon$ around ε).

The atoms in InP crystallise in a zinc-blend structure. Like most III-V semiconductors, a simplified 3 valley band structure may be used. This model treats the conduction band as a combination of the Γ, X and L valleys that are discrete, or separate from each other. The three valleys are treated as non-parabolic valleys. A simple analytical way of introducing non-parabolicity is to consider an energy-wave vector relation of the type:

$$\begin{aligned} \varepsilon(1 + \alpha\varepsilon) &= \frac{\hbar^2 k^2}{2m} = \gamma(k) \\ \varepsilon(k) &= \frac{-1 + \sqrt{1 + 4\alpha\gamma(k)}}{2\alpha} \end{aligned} \tag{10}$$

where α is a non-parabolicity parameter.

The scattering mechanisms taken into account were acoustic phonon, polar and non-polar optic phonons and intervalley (Γ⇔L, Γ⇔X, L⇔X, with the absorption/emission of one or two phonons). Piezoelectric scattering has a negligible effect at 300 K. Inter-carrier scattering (electron-electron and electron-hole) is also neglected. The parameters used in the simulation are shown in table 1 [7,8].

Table 1: InP parameters used in the MC simulation.

Parameter	Γ	L	X
Polar optic phonon energy (eV)	0432	0.0432	0.0432
Non-polar optic phonon energy (eV)	0.043	0.043	0.043
Non-polar optic deformation potential (eV/m)	$67x10^{10}$	$67x10^{10}$	$67x10^{10}$
Acoustic potential (eV)	7	12	11
Intervalley: phonon 1		$1.37x10^{11}$	$1.25x10^{11}$
Deformation potential (eV/m) Γ →		0.0337	0.0337
Energy (eV)	$1.37x10^{11}$	$5.6x10^{10}$	$8.4x10^{10}$
Deformation potential (eV/m) L →	0.0337	0.0337	0.0337
Energy (eV)	$1.25x10^{11}$	$8.4x10^{10}$	$9.9x10^{10}$
Deformation potential (eV/m) X→	0.0337	0.0337	0.0239
Energy (eV)			
Intervalley: phonon 2		$1.4x10^{10}$	$7.5x10^{9}$
Deformation potential (eV/m) Γ →		0.0068	0.0084
Energy (eV)	$1.4x10^{10}$		$1.94x10^{10}$
Deformation potential (eV/m) L →	0.0068		0.0068
Energy (eV)			
Deformation potential (eV/m) X→	$7.5x10^{9}$	$1.94x10^{10}$	$1x10^{5}$
Energy (eV)	0.0084	0.0068	0.0128

II- SIMULATION RESULTS & DISCUSSION

A- Transient response

The simulation of electron transport phenomena in undoped InP at 300 K is performed using the method described above. Initial conditions are very important in the simulation of transient regime, in order to build an initial energy distribution. We first started with a Maxwellian carrier distribution and the system was left to drift for 10 picoseconds under zero electric field. The obtained electron distribution was not a Maxwellian.

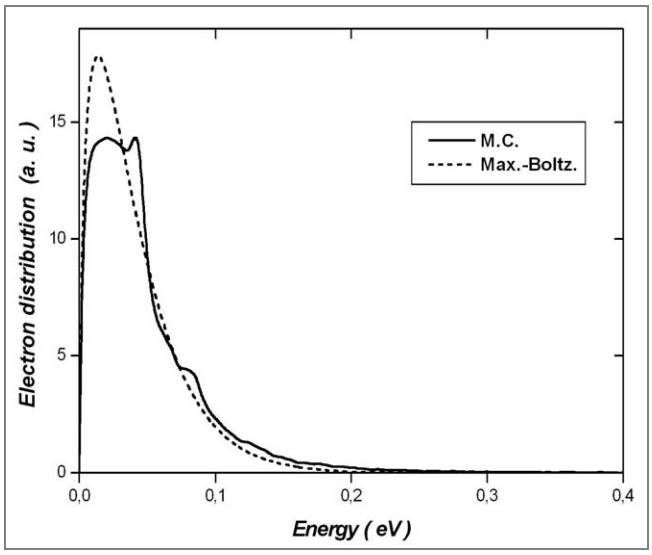

Figure 1: Initial electron distribution in undoped InP at T= 300 K with Maxwell- Boltzmann distribution.

Figure 1 shows that an important peak appears at 39 meV, which agrees well with the expected value of $3/2k_BT$ at T = 300 K. The second peak, less important, is found around 43 meV and is due to the absorption of optical phonons $\hbar\omega_{op}$ = 43.2 meV. This energy distribution was taken as the initial distribution throughout this work.

The applied electric field is assumed constant and uniform. As we only work in momentum space, the actual geometrical position of the particles need not be calculated.

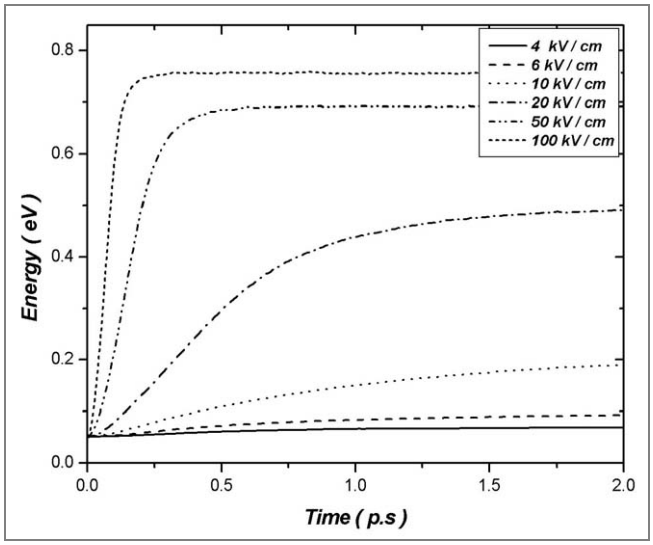

Figure 2: The transient response of mean energy of electrons in InP to different uniform electric fields.

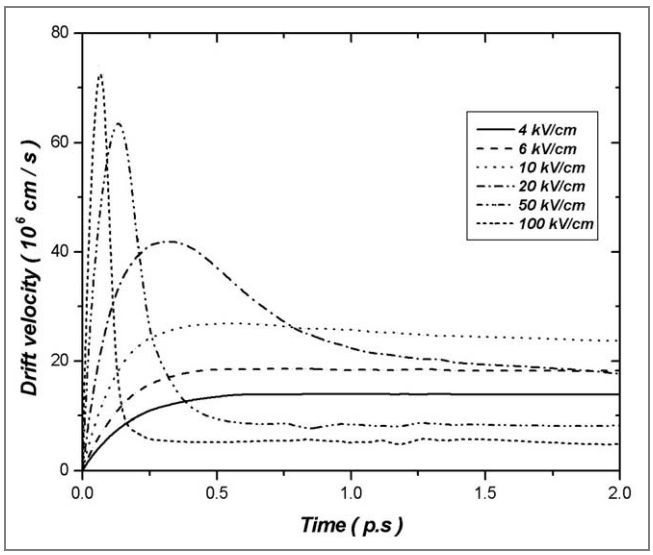

Figure 3: The transient response of average drift velocity of electrons in InP to different uniform electric fields.

The response of the electron gas to an applied electric field takes time. In macroscopic theory it is expressed through the momentum and energy relaxation times. From figures 2 and 3 we can make the distinction between momentum and energy relaxation. The latter shows that the drift velocity increases to much initially, before relaxing to its steady state value. The reason for this is that the field first accelerates the particles; these faster particles are then

subjected to increased scattering resulting in a net loss of energy to the lattice. For higher electric fields the electrons begin to increase in energy and move up the valleys. In higher valleys, due to the fact that the velocity is inversely proportional to the effective masse, the velocity will decrease as the masses increase. Once in the valleys, the velocities begin to decrease until the valley to valley scattering rates and phonon scattering rates reach equilibrium and saturation is met. This is the velocity overshoot effect which is observed in almost all III-V compounds. The velocity overshoot is observed in InP for fields exceeding 10 *kV/cm*.

Figure 4 shows the variation of energy and momentum relaxation times. The values are calculated from the *v(t)* and ε(*t*) using a non-linear least squares fitter. For low electric fields, the calculation of the energy relaxation time error was important as the energy was close to the equilibrium value. The error for both energy and momentum relaxation times was in all cases less than 5%. The energy relaxation curve consists of two regions. In the first one, the relaxation time increases with the electric field up to ~10 *kV/cm*, since the energy gained by the electrons could not be dissipated rapidly. In the second region it falls down sharply. The first increase could be attributed to active scattering mechanisms, where the electron needs longer time to dissipate the energy gained from the electric field during the free flight. As the energy gained by the electron increases, the rate of more effective energy dissipating scattering mechanisms is increased, essentially the intervalley scattering. Therefore leading to a considerable diminution of the relaxation time. The momentum relaxation time shows an exponential decay with the electric field. Its value is generally much reduced than that of the energy relaxation time.

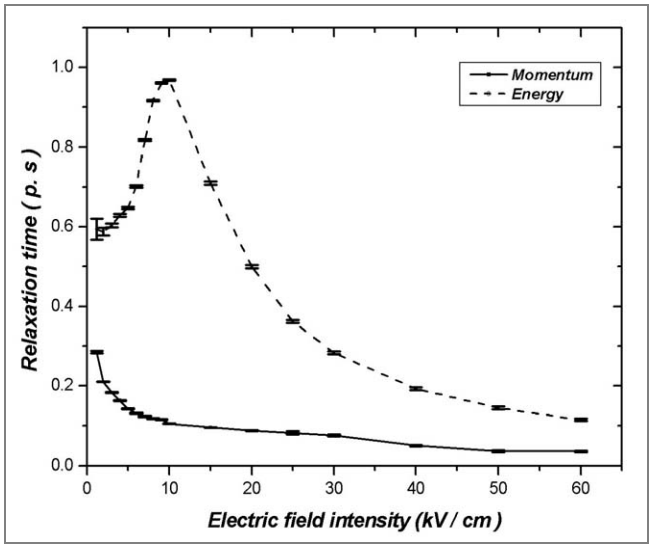

Figure 4: Energy and momentum relaxation times of electrons as a function of electric field strength.

B- Steady state regime

The dependence of the electron drift velocity on the applied field is one of the most important relations required in the physical models and numerical simulations of semiconductor devices. In figure 5 the mean drift velocity curve shows a maximum of about 2.31x10^7 *cm/s* at a critical

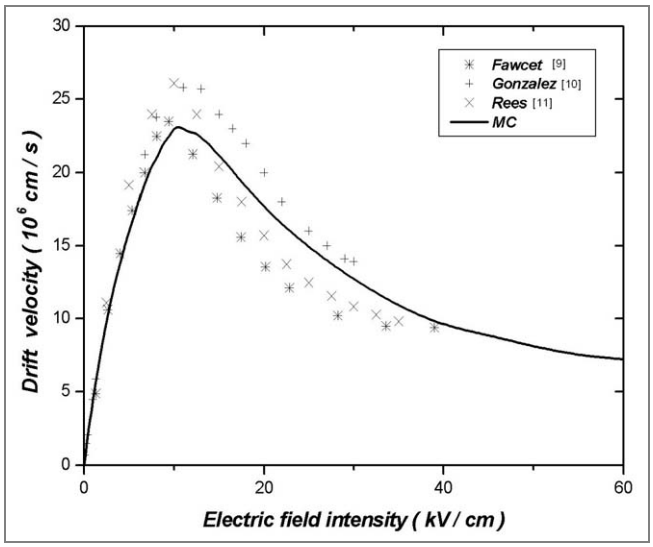

Figure 5: Drift velocity of electrons as a function of field strength.

field of ~10.5 *kV/cm*. For higher fields it decreases to saturates near 7.2 x10^7 *cm/s*. For low electric field values, the velocity increases linearly with the electric field following an expression of the form: $v(E) = \mu E$ where μ stands for the mobility. With further increase in the electric field, the electron drift velocity decrease. This phenomena, known as the negative differential mobility, has been observed in many III-V compound semiconductors. As mentioned above, the decrease of the drift velocity is due to the scattering of electrons into higher valleys, L and X (for very high electric fields above 40 *kV/cm*) where the mobility is low. The obtained curve fits well with the reported results of Fawcet *et al.* [9], Gonzalez *et al.* [10] and Rees et al [11]. Figure 6 represents the variation of the mobility (*v(E)/E*) for electric fields below 4 kV/cm. The mobility is nearly constant with a value of 47026 ± 34 *cm^2/Vs* which compares very well with reported experimental value at 300 K [12]. For intense electric fields the mobility decreases remarkably, below 100 *cm^2/Vs* for E ~ 60 *kV/cm*.

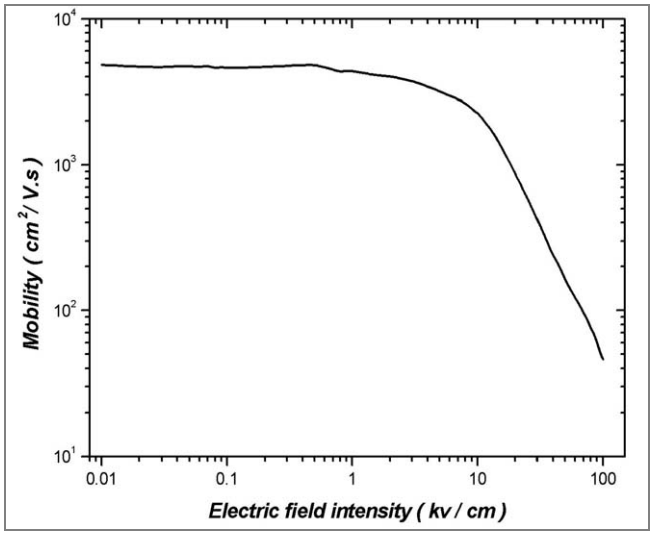

Figure 6: Electrons mobility as a function of field strength.

The mean energy exhibit a parabolic increase with the electric field for lower values of E (Fig. 7). For high electric field the mean energy increase is less remarkable and a saturation is obtained. Initially all electrons are in the central valley Γ at 300 K. As the electric field increases continuous migration of electrons into the L valley takes place. If the electric field is high enough, the scattering into the X valley is observed too. In figure 8 the evolution of population occupancy is represented for different intensities of the electric field. The simulated results are in good agreement with those reported by Borodovskii et al [13]. For intense E there is growing disagreement with Borodovskii *et al*. We think that it may be induced by the use of analytical (non-parabolic) dependence of the energy in the scattering rates calculation.

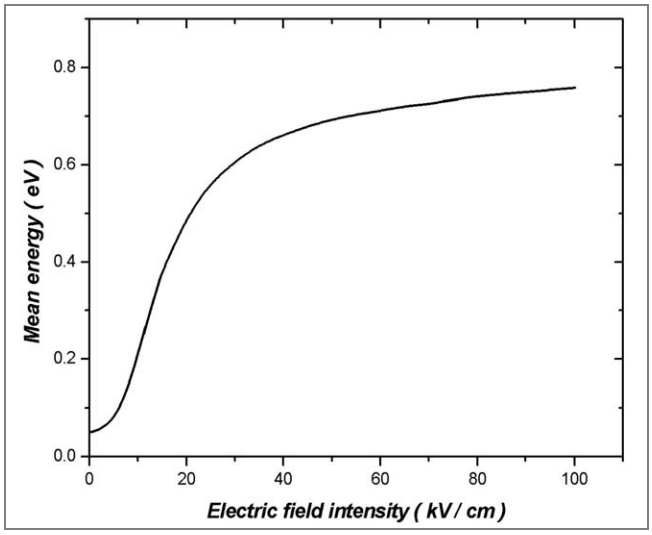

Figure 7: Average energy of electrons as a function of field strength.

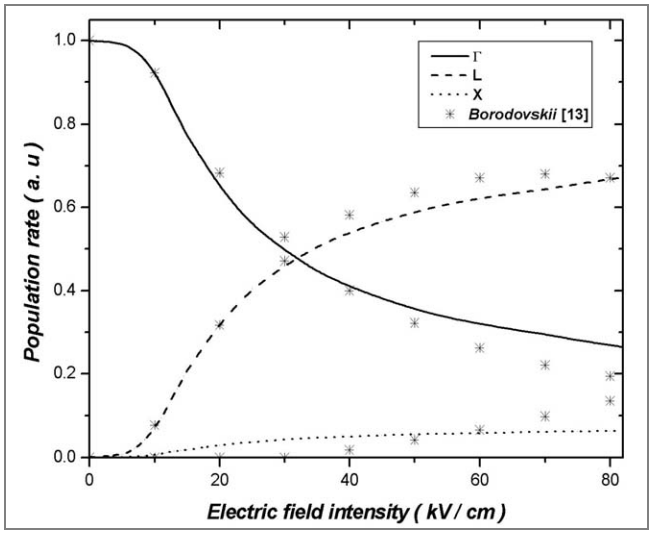

Figure 8: Population ratio in valleys Γ, X and L of electrons as a function of field strength.

The initial energy distribution in figure 1 was used in the simulation where all electrons are in the central Γ valley at zero electric field. It is reported that the choice of the initial state is not important in steady state simulation, unlike the transient regime where it is very decisive. Figure 9 illustrates the effect of the electric field on the steady state distribution function. For low electric fields (< 5 *kV/cm*) the distribution function could be approximated to the Maxwell-Boltzmann distribution in the central valley. As the electric field increases (above 10 *kV/cm*), a second peak corresponding to the L valley appears at energies around 0.61 *eV* while the first Γ peak diminishes. When the electric field is increased further (above 40 *kV/cm*) a third peak comes into view corresponding to the X valley, whereas the L peak becomes very important too.

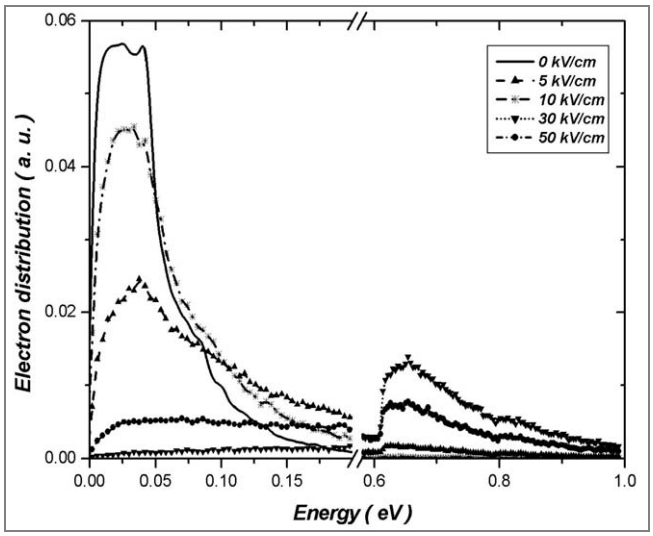

Figure 9: The effect of electric field on the steady state electron distribution in InP at 300 K.

From this figure we can justify the assumption that at 300 K all electrons are supposed in the Γ valley. It can also be seen that at any voltage the electron population from the three valleys contribute to the transport phenomena. This is important in the determination of the transport parameters as each fraction of the population has its own effective masse and therefore its mobility.

CONCLUSION

We presented a description of the Monte Carlo modelling of transient and steady state regimes in bulk InP. The basic improvement of the algorithm was to reduce enormously the calculating time by introducing the iterative Gamma approach. This technique reduces the rate of self scattering which is a time consuming procedure. We arrived to build an initial energy distribution, different from a Maxwell-Boltzmann distribution, that gives better transient regime response. Using a simple non-parabolic analytical dispersion relations $\varepsilon(k)$ it was possible to produce fairly accurate results for moderately high electric fields. At very high electric field intensities the proposed method shows some limitations. Indeed, when the energy of electrons reach

values above 2 eV the scattering rates obtained by the non-parabolic model is no longer valid. The obtained results could be the basis of more sophisticated device modelling techniques.

REFERENCES

[1]- Vasileska D. and Goodnick S.M., *Materials Science and Engineering*, R38 (2002), p.181.

[2]- Suchecka M**.**, *Materials Science Forum*, Vol.297-298, (1999), p.279.

[3]- Jacoboni C. and Reggiani L., *Review of Modern Physics*, Vol.55, N°3, (1983), p.645.

[4]- Jacoboni C. and Lugli P., *The Monte Carlo method for semiconductor device simulation*, Springer-Verlag/Wien, (1989).

[5]- Rees H.D., *Phys. Lett*. A, Vol. 26, (1968), p.416.

[6]- Moglestue C., *Monte Carlo simulation of semiconductor devices*, Chapman & Hall London, (1993).

[7]- Vaissiére J.C., Elkssimi M. and Nougier J.P., *Semicond. Sci. Technol.*, 7, (1992), p.B308.

[8]- Gasquet D., thèses de Doctorat d'Etat, Languedoc, Montpellier, (1984).

[9]- Fawcet W. and Hill G., *Electron. Lett*. **11**, 4, (1975), pp.80-81.

[10]- Gonzalez S.T., Velazquez J.E.P., Gutierrez P.M.C. and Pardo D., *Semicond. Sci. Technol*., 7, 1, (1992), pp.31-36

[11]- Rees H.D. and Gray K.W., *Solid St. Electron. Devices* 1, (1976), p.1.

[12]- Sze S.M., *Physics of Semiconductor Devices*, 2nd Edition, Wiley-interscience Publication, (1981).

[13]- Borodovskii P.A. and Osadchi V.M., *Intervalley transfer of Electron in A_{III}-B_V Semiconductors*, Inst. Of Semiconductor Physics, Novosibirsk, (1987), p.170 (in Russian). □